HOSTED BY

ELSEVIER

CrossMark

Available online at www.sciencedirect.com

ScienceDirect

Journal of Magnesium and Alloys 3 (2015) 162−167
www.elsevier.com/journals/journal-of-magnesium-and-alloys/2213-9567

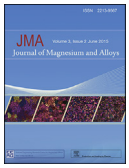

Full length article

Processing, microstructure and mechanical properties of bimodal size SiCp reinforced AZ31B magnesium matrix composites

M.J. Shen [a,*], M.F. Zhang [b], W.F. Ying [c]

[a] College of Engineering, Shenyang Agricultural University, Shenyang 110866, PR China
[b] Liaoning Provincial Gem Quality Supervision and Inspection Center, Shenyang 110000, PR China
[c] College of Chemical Engineering and Materials Science, Eastern Liaoning University, Dandong 118003, PR China

Received 8 February 2015; accepted 8 May 2015
Available online 20 June 2015

Abstract

The bimodal size SiC particulates (SiCp) reinforced magnesium matrix composites with different ratios of micron SiCp and nano SiCp (M-SiCp:N-SiCp = 14.5:0.5, 14:1, and 13.5:1.5) were prepared by semisolid stirring assisted ultrasonic vibration method. The AZ31B alloy and all as-cast SiCp/AZ31B composites were extruded at 350 °C with the ratio of 12:1. Microstructural characterization of the extruded M14 + N1 (M-SiCp:N-SiCp = 14:1) composite revealed the uniform distribution of bimodal size SiCp and significant grain refinement. Optical Microscopy(OM) observation showed that, compared with the M14.5 + N0.5 (M-SiCp:N-SiCp = 14.5:0.5) composite, there are more recrystallized grains in M14 + N1 (M-SiCp:N-SiCp = 14:1) and M13.5 + N1.5 (M-SiCp:N-SiCp = 13.5:1.5) composites, but in comparison to the M13.5 + N1.5 composite, the average grain size of the M14 + N1 composite is slightly decreased. The evaluation of mechanical properties indicated that the yield strength and ultimate tensile strength of the M14 + N1 composite were obviously increased compared with other composites.

Keywords: Magnesium matrix composite; Microstructure; Mechanical properties

1. Introduction

The SiCp reinforced magnesium matrix composites (MMCs) have obtained superior mechanical and physical properties in comparison to the unreinforced alloy, such as high specific strength, high hardness, well wear resistance and low coefficient of thermal expansion (CTE). Therefore, many research works about the preparation methods and processing technique of the SiCp reinforced metal matrix composites have been published in recent years. In general, the SiCp reinforced magnesium matrix composites are fabricated by disintegrated melt deposition, expensive powder metallurgy, friction stir processing and mechanical milling methods.

Single and various sizes SiCp reinforced magnesium matrix composites are considered as excellent structural materials to be applied in the aerospace and automobile industry. Moustafa [1] had successfully prepared aluminium matrix composites reinforced with various sizes of SiCp by squeeze casting method under the protection of argon gas. Moreover, he also found that the large-sized particles reinforced composites had much lower porosity density, higher relative density and superior mechanical properties comparing with the small-sized particles reinforced composites, which can be ascribed to the good interface bonding between the matrix and the reinforcement. Deng et al. [2] fabricated the submicron-SiCp/AZ91 magnesium matrix composites by using stir casting

* Corresponding author. Tel./fax: +86 2431530612.
E-mail addresses: smjiekaka@163.com (M.J. Shen), yingweifengneu@163.com (W.F. Ying).
Peer review under responsibility of National Engineering Research Center for Magnesium Alloys of China, Chongqing University.

http://dx.doi.org/10.1016/j.jma.2015.05.002.

method, and found that the addition of submicron-SiCp(2 vol.%) led to a simultaneous improvement in the thermal stability, micro-hardness, elastic modulus and 0.2% yield strength. Wang et al. [3] fabricated the 10 vol.%SiCp/Mg−Zn−Ca composites by using stir casting method, and found that the addition of micron-SiCp resulted in significant improvement on tensile properties of Mg−Zn−Ca alloy due to the coefficient of thermal expansion mismatch between the matrix and the particles, effective load transfer and Hall−Petch strengthening mechanisms. Therefore, we can know that the addition of SiCp has a significant effect on the mechanical properties and microstructures of the metal matrix composites. In fact, our previous works have shown that the mechanical properties and damping capacities of the matrix alloys reinforced with micron or nano SiCp were greatly improved [4−6]. The above-mentioned considerations have led us to conceive a magnesium matrix composite reinforced with bimodal size SiC particles, and recently our work has suggested that the superior mechanical properties were obtained in the micron and submicron SiCp reinforced magnesium matrix composites [7]. However, so far there are still no detailed works have been reported about the influence of micron and nano bimodal sizes SiCp on microstructures and mechanical properties of MMCs. Therefore, our present main work is to study the effect of volume ratios of micron SiCp and nano SiCp on the microstructures and mechanical properties of bimodal size SiCp/AZ31B composites, and explain the strengthening reason of the bimodal size SiCp/AZ31B composites.

2. Experimental procedure

An ingot of AZ31B magnesium alloy with a nominal composition of Mg-2.8Al-0.8Zn-0.3Mn was used as the matrix alloy, and two sizes of SiC particles (nano and micron) were employed as the reinforcements in the present work. The average sizes of micron and nano SiC particles (respectively denoted as “M-SiCp and N-SiCp”) are about 10 μm and 60 nm. Three kinds of designations for the bimodal size SiCp/AZ31B composites were summarized in Table 1. The bimodal size SiCp reinforced AZ31B magnesium matrix composites were fabricated with a molten metal of magnesium by semi-solid stirring assisted ultrasonic vibration method. In each experiment, about 1 kg of AZ31B alloy were first melt at 720 °C and then cooled to 620 °C. Subsequently, the micron and nano SiC particles were added into semi-solid melt, the molten slurry of SiCp and the AZ31B alloy was stirred in a protective atmosphere of CO_2 and SF_6 to avoid burning. After semisolid stirring for 10 min, the mixture of melt and bimodal size SiCp was rapidly reheated to 720 °C, and then the slurry was ultrasonically processed at 500 W power level for 20 min before removing the ultrasonic probe from the melt. After the ultrasonic vibration, the melt mixture of SiCp and the AZ31B alloy was poured into a preheated steel mould (450 °C) and allowed to solidify under 100 MPa pressure to obtain bimodal size SiCp/AZ31B composite ingots without porosity. The cast billets were homogenized at 400 °C for 12 h before hot extrusion, and then produced about 25 cm of rods at 350 °C with an extrusion ratio of 12:1.

Table 1
Composites designations.

Micron SiCp (vol.%)	Nano SiCp (vol.%)	Designation
14.5	0.5	M14.5 + N0.5
14	1	M14 + N1
13.5	1.5	M13.5 + N1.5

The microstructures of the samples were observed by using Optical Microscopy (OM) (PMG-3, Olympus, Japan), Scanning Electron Microscope (SEM) (Quanta 200FEG, FEI Co.Ltd., USA) and Transmission Electron Microscopy (TEM) (HR-TEM, Tecnai G^2 F30, USA). The phase compositions of the SiCp/AZ31B composite, reinforcement and AZ31B alloy were examined with X-ray Diffraction (XRD) (D/max-rB, Rigaku, Japan) using a Cu Kα source. For the SEM and OM study, the specimens were sectioned parallel to extrusion direction and prepared by the conventional mechanical grinding, polishing and etched in acetic picral [2 ml acetic acid + 2 g picric acid + 20 ml ethanol (95%)]. The average grain size of each sample was obtained by using the mean linear intercept method. The room temperature tensile tests were carried out on an Instron Series 5569 test machine with the tensile rate of 0.5 mm/min. In this experiment, the average tensile data of each sample were obtained from 3 to 5 tests at the same condition. The dimensions of tensile specimens were given in our previous work [4].

3. Result and discussion

3.1. Phase composition analysis

Fig. 1 shows the X-ray diffraction patterns of the AZ31B alloy, reinforcement and SiCp/AZ31B composite. According to the XRD patterns, compared with the ASTM cards, it can be concluded that the micron SiC particle is α-SiCp with hexagonal structure, while nano SiC particle is β-SiCp with face

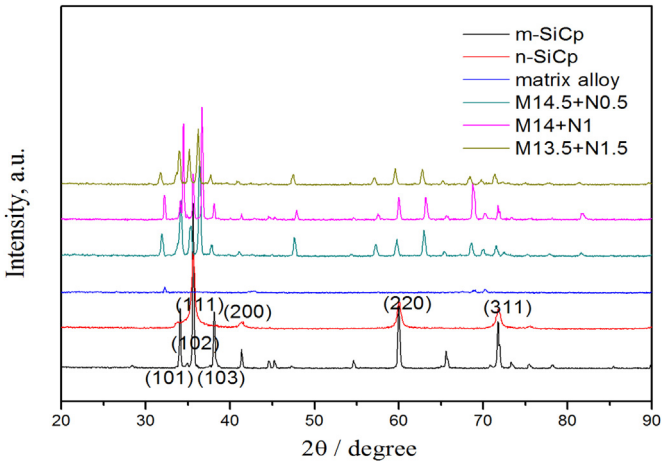

Fig. 1. XRD patterns of SiCp, matrix alloy and SiCp/AZ31B composites.

centered cubic structure. No matter how much the nano SiCp content is, the bimodal size SiCp/AZ31B composite is only composed of Mg and α-SiC phases. The intensity of peaks corresponding to the AZ31B alloy and M-SiCp is very strong. Unexpectedly, as the main part of the bimodal size SiCp/AZ31B composites, no peaks associated with β-SiCp appear in the XRD pattern. This is probably due to XRD can only detect compositions of phases present at concentrations greater than 5%.

3.2. Microstructure observation

Fig. 2 shows the optical micrographs of the monolithic AZ31B alloy and bimodal size SiCp/AZ31B composites after hot extrusion. Fig. 3 shows the average grain sizes of the AZ31B alloy and bimodal size SiCp/AZ31B composites. Compared with the AZ31B alloy, the grain sizes of all the as-extruded bimodal size SiCp/AZ31B composites are much smaller. This indicates that the addition of the bimodal size SiCp has a significant influence on reducing grain size of the matrix. When the total volume fraction of SiCp is 15%, the grains of the M14 + N1 and the M13.5 + N1.5 composites are much finer than that of the M14.5 + N0.5 composite. However, in comparison to the M13.5 + N1.5 composite, the average grain size of the M14 + N1 composite is slightly decreased. This reveals that the grain size of the matrix in the bimodal size SiCp/AZ31B composites firstly decreased and then increased when the volume fraction of nano SiCp increased from 0.5 vol.% to 1.5 vol.%. Moreover, the presence of finer equiaxed grains indicates that the dynamic recrystallization (DRX) occurred in the bimodal size SiCp/AZ31B composite during hot extrusion. Compared with the M14.5 + N0.5 composite, the DRX grains of the M14 + N1 and the M13.5 + N1.5 composites become much fuller, and the scale of grain size distribution is reduced, as shown in Fig. 2(c) and (d). However, the fine-grained and large-grained zones between the SiCp can be observed in the M13.5 + N1.5

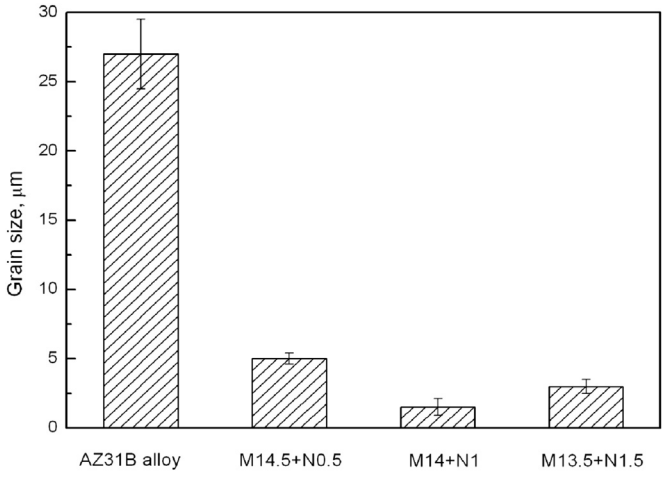

Fig. 3. Grain sizes of AZ31B alloy and SiCp/AZ31B composites after hot extrusion.

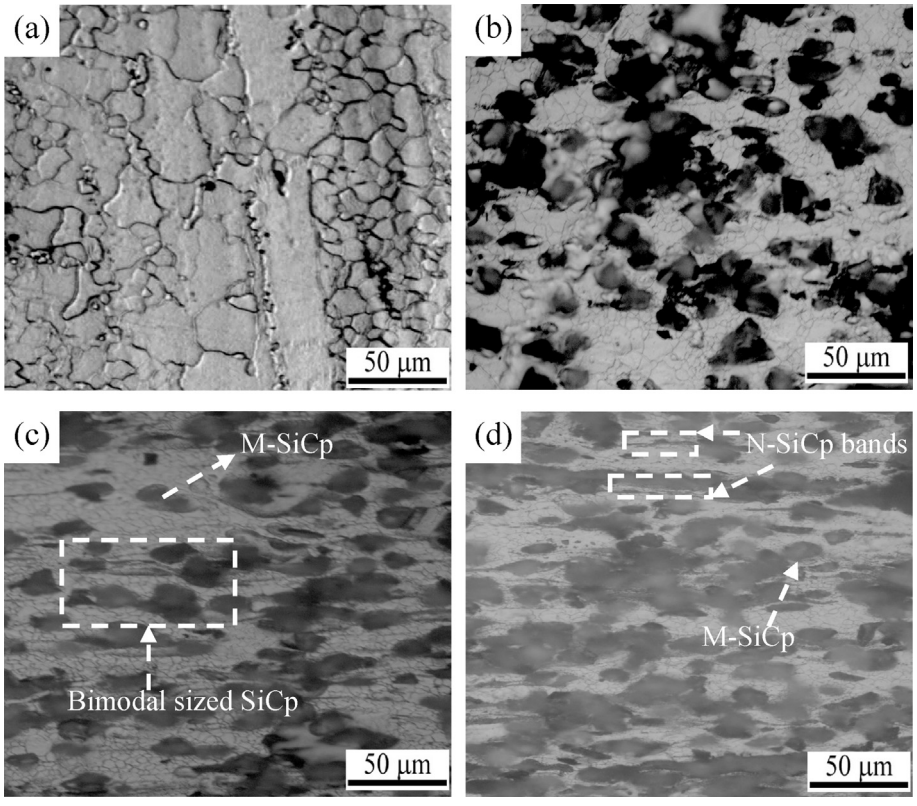

Fig. 2. Optical micrographs of as-extruded alloy and SiCp/AZ31B composites. (a) AZ31B alloy, (b) M14.5 + N0.5 composite, (c) M14 + N1 composite, (d) M13.5 + N1.5 composite.

composites. When the nano SiCp content is 1 vol.%, the average size of the obtained grains is the smallest in the present composites, which can be explained as follows: (1) The addition of nano SiCp has a significant pinning effect on grain boundary, which can inhibit or delay the recrystallization grain growth of the matrix. (2) The size of nano SiCp is obviously smaller than the size of micron SiCp. Therefore, With the increase of nano SiCp volume fraction, the amount of SiCp also increased when the total volume fraction of SiCp is 15%, which can introduce the larger driving force and much more stored energy to promote DRX nucleation of matrix [8]. As a result, this can effectively restrict the grain growth during the hot extrusion. When the volume fraction of nano SiCp increased to 1.5%, the agglomeration zones appeared, and the average grain size of the M13.5 + N1.5 composite was slightly increased. However, the N-SiCp cannot be clearly found because of the lower magnification. Therefore, the SEM analysis is required in this present work, as shown in Fig. 4. This will result that the average grain size of the M13.5 + N1.5 composite was slightly larger than that of the M14 + N1 composite in present work. (3) The added micron SiCp may stimulate nucleation at the early stage of deformation and then restrict the grain growth during the hot deformation [9]. In addition, we can observe that the sizes of grains around micron SiCp are smaller than that far away from micron SiCp zones. The reason is that the large-sized micron SiCp are favourable to grain refinement by promoting DRX nucleation [7].

Some researchers have published about the effect of particle sizes on DRX during hot deformation. The M-SiCp could stimulate dynamic recrystallization of magnesium alloy during hot extrusion, which caused the obvious grains refinement [10]. However, the N-SiCp (~60 nm) could delay or hinder recrystallization of magnesium alloy, which was due to the pin grain boundary effect of finer particles (<1 μm) during hot deformation [11]. We previous work also has indicated the same conclusion on submicron-SiCp reinforced AZ91D magnesium matrix composite [12]. In the present researches, the grains of bimodal size SiCp/AZ31B composites have been significantly refined. This can be attributed to the recrystallization nucleation of M-SiCp and the pinning effect of N-SiCp.

The SEM graphs of the bimodal size SiCp/AZ31B composites at low and high magnification are shown in Fig. 4. The white and grey phases represent M-SiCp and the matrix at low magnification, respectively. It can be seen that the distribution of micron SiCp becomes relative homogeneous in the bimodal size SiCp/AZ31B composites at low magnification, which suggests that the hot extrusion has a significant effect on improving the distribution of M-SiCp. The reason for such homogeneous distribution of particles is that the hot extrusion can impel the matrix flow into the reinforcement clusters. This because of flow velocity of the matrix is faster than that of M-SiCp. From Fig. 4 it also can be seen that most of SiC particles were distributed along the extrusion direction, this reason may be that the strong plastic deformation of the matrix impel SiCp to distribute along the extrusion direction during hot extrusion. The morphology and the distribution of N-SiCp in the SiCp/AZ31B composites are shown in high magnification graphs. With increasing the volume fraction of N-SiCp, the amount of N-SiCp was gradually increased. It can also be found that the N-SiC particles were homogeneous distributed in the matrix when nano SiCp content did not overrun 1 vol.%, as shown in Fig. 4(d) and (e). However, the particles cluster zone and the N-SiCp rich region appeared with the volume fraction of N-SiCp increased to 1.5%, as shown in Fig. 4(f). Compared with the M14.5 + N0.5 and the M14 + N1 composites, the wettability between the N-SiCp and the matrix in the M13.5 + N1.5 composite is poor, as shown in higher magnification SEM micrograph (in Fig. 4(f)). It illustrates that the poor interfacial bonding existed between the N-SiCp and the

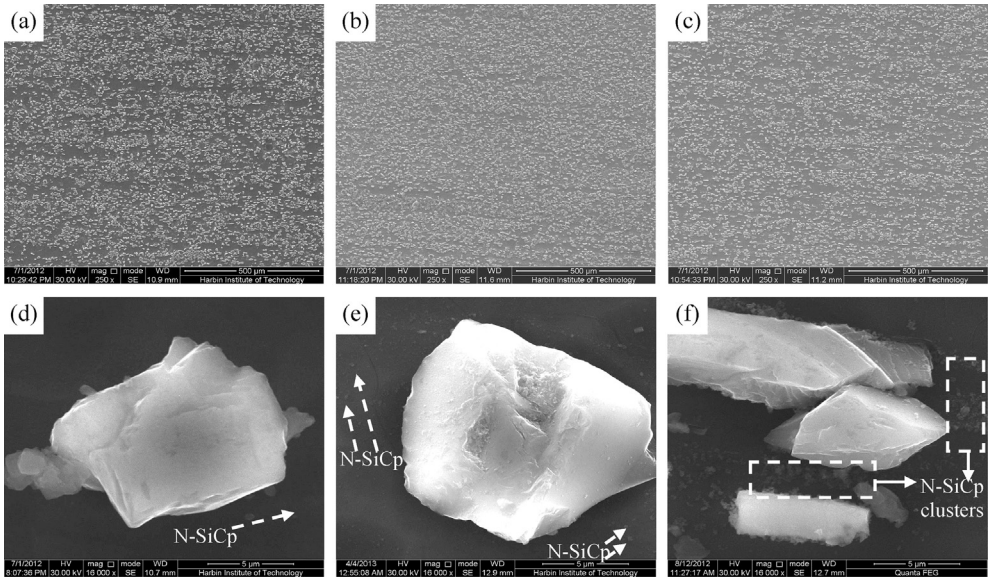

Fig. 4. SEM micrographs of as-extruded SiCp/AZ31B composites. (a) M14.5+N0.5 composite, (b) M14+N1 composite, (c) M13.5+N1.5 composite, (d) high magnification of (a), (e) high magnification of (b), (f) high magnification of (c).

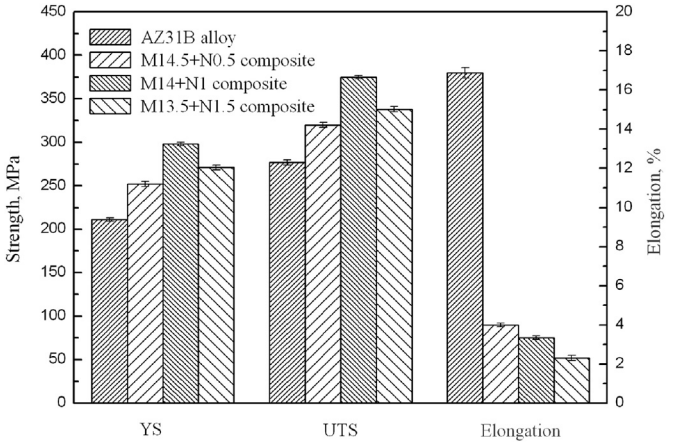

Fig. 5. Tensile properties of AZ31B alloy and SiCp/AZ31B composites after hot extrusion.

matrix in the M13.5 + N1.5 composite. Moreover, when the volume fraction of N-SiCp increased to 1.5%, the agglomerating of nano SiCp causes the rich of micron SiCp. The images are shown in Fig. 4(f).

3.3. Mechanical properties

The tensile properties of the AZ31B alloy and bimodal size SiCp/AZ31B composites after hot extrusion are shown in Fig. 5. Compared with the AZ31B alloy, the yield strength and ultimate tensile strength of the bimodal size SiCp/AZ31B composites were obviously increased, while the elongation to fracture was decreased. The enhancement of yield strength is mainly attributed to the low degree of porosity, relative homogeneous distribution of particles and grain refinement which lead to transfer of applied tensile load to the SiCp in the present work.

It also can be found from Fig. 5 that the yield strength and ultimate tensile strength of bimodal size SiCp/AZ31B composites firstly increased and then decreased with increasing the content (vol. %) of nano SiCp when the total volume fraction of SiCp is 15%. It could be attributed to the significant grain refinement when 1 vol.% of nano SiCp were added. The decrease of grain size leads to increasing the yield strength of the matrix, which can be described by Hall–Petch relation [13]: $\sigma_y = \sigma_0 + Ky/d^{1/2}$, where σ_0 and Ky are material constants, d is the average grain size, and σ_y is the yield strength. In addition, the multidirectional thermal stress generated at the interface between the particle and the matrix, this is attributed to the great difference on coefficient of thermal expansion (CTE) berween the SiCp and the matrix. And the addition of micron and nano SiCp may induce high dislocation density in the composite [14,15]. The above reasons lead to the increase of the yield strength in the bimodal size SiCp/AZ31B composites. However, the yield strength value of the SiCp/AZ31B composite was reduced when the volume fraction of nano SiCp increased from 1 vol.% to 1.5 vol.%. This could be attributed to the significant increase of the agglomerating zones with the nano SiCp content further increased, as shown in Fig. 4(f). We previous work has reported that SiCp

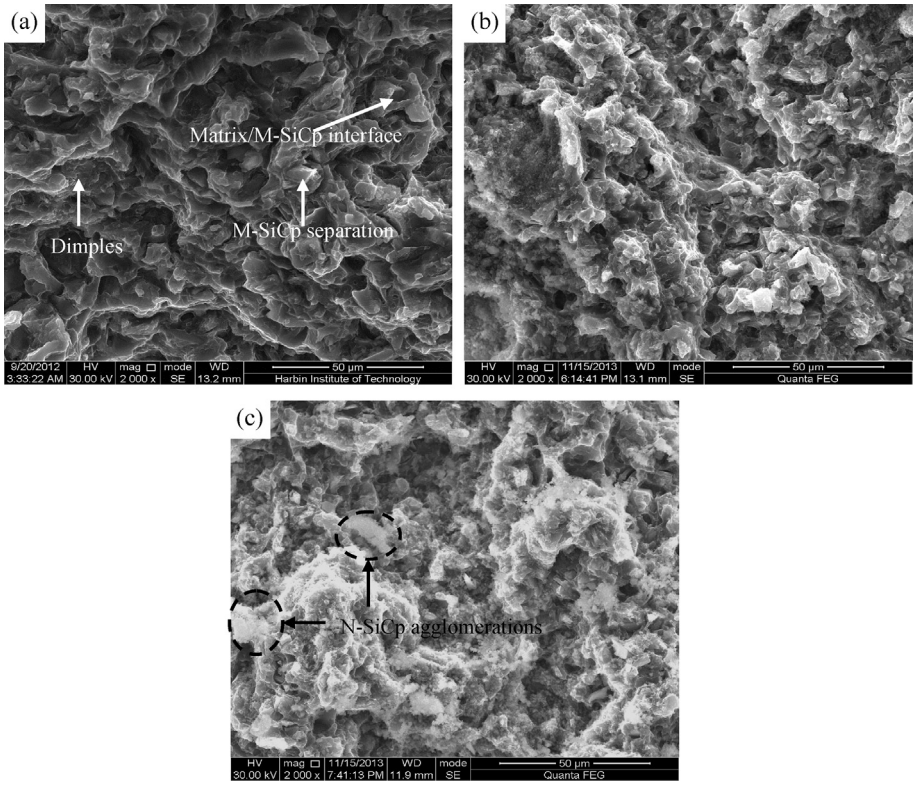

Fig. 6. Fracture surface of the SiCp/AZ31B composites. (a) M14.5 + N0.5 composite, (b) M14 + N1 composite, (c) M13.5 + N1.5 composite.

agglomeration would weak the strengthened effect of the reinforcements [16]. Moreover, the poor interfacial bonding and wettability appeared when nano SiCp content increased from 1 vol.% to 1.5 vol.%, which is also the reason for reducing the yield strength of the matrix.

3.4. Fracture observation

The fracture surface of bimodal size SiCp/AZ31B composites is shown in Fig. 6, it indicates that the composites brittle fractured during room temperature tensile. The relatively low strain as seen in the tensile properties (Fig. 5) is the indication of the premature failure due to interface debonding between the M-SiCp and matrix. Many debonded M-SiCp are present on the fracture surface of composite, which are the main reasons for poor ductility of the SiCp/AZ31B composites in the present work. Therefore, the interface debonding of M-SiCp results in the brittle fracture of the bimodal size SiCp/AZ31B composites. Moreover, N-SiCp clusters as shown in Fig. 6(c) also is the main reasons for fast failure, which leads to poor mechanical properties of the M13.5 + N1.5 composite. The SEM observation on the fractured surfaces of the M13.5 + N1.5 composites is consistent with the obtained distribution of N-SiCp given in the previous section.

4. Conclusions

The influence of volume ratio of bimodal size SiCp on microstructures and mechanical properties of the SiCp/AZ31B composites fabricated by semisolid stirring assisted ultrasonic vibration was investigated, and the main conclusions can be summarized as follows:

(1) The addition of bimodal size SiCp leads to the significant refinement of the matrix grains in the SiCp/AZ31B composite. Compared with the M14.5 + N0.5 composite, the DRX of the M14 + N1 and the M13.5 + N1.5 composites become much fuller, and the size of the grains is also reduced. However, the average grain size of the M14 + N1 composite is slightly decreased compared with the M13.5 + N1.5 composite.
(2) The nano SiC particles were homogeneous distributed in the matrix when the nano SiCp content did not overrun 1 vol.%. However, the particles cluster zone and the N-SiCp rich region appeared with the volume fraction of the N-SiCp increased to 1.5%.
(3) Both of the yield strength and ultimate tensile strength firstly increased and then decreased with the increase of nano SiC particles volume fractions, while the elongation to fracture was gradually decreased when the total volume fraction of SiCp is 15%.
(4) The increase in the yield strength of the bimodal size SiCp/AZ31B composites is attributed to the uniform distribution of the bimodal size SiCp and the obvious grain refinement, while this grain refinement is caused by the combination effect of the dynamic recrystallization and the pinning effect on grain boundary.

References

[1] S.F. Moustafa, Z. Abdel-Hamid, A.M. Abd-Elhay, Mater. Lett. 53 (2002) 244−249.
[2] K.K. Deng, K. Wu, Y.W. Wu, K.B. Nie, M.Y. Zheng, J. Alloys Compd. 504 (2010) 542−547.
[3] X.J. Wang, K.B. Nie, X.S. Hu, Y.Q. Wang, X.J. Sa, K. Wu, J. Alloys Compd. 532 (2012) 78−85.
[4] K.K. Deng, K. Wu, X.J. Wang, Y.W. Wu, X.S. Hu, M.Y. Zheng, W.M. Gan, H.G. Brokmeier, Mater. Sci. Eng. A 527 (2010) 1630−1635.
[5] H. Ferkel, B.L. Mordike, Mater. Sci. Eng. A 298 (2001) 193−199.
[6] B.W. Chua, L. Lu, M. Lai, Compos. Struct. 47 (1999) 595−601.
[7] K.K. Deng, C.J. Wang, X.J. Wang, Y.W. Wu, K.B. Nie, K. Wu, Composites Part A 43 (2012) 1280−1284.
[8] V. Kevorkuan, Mater. Sci. Tech. 19 (2003) 1386−1390.
[9] J. Lan, Y. Yang, X.C. Li, Mater. Sci. Eng. A 386 (2004) 284−290.
[10] X.J. Wang, K.B. Nie, X.S. Hu, X.J. Sa, K. Wu, M.Y. Zheng, Mater. Sci. Eng. A 534 (2012) 60−67.
[11] K.B. Nie, X.J. Wang, X.S. Hu, L. Xu, K. Wu, M.Y. Zheng, Mater. Sci. Eng. A 528 (2011) 5278−5282.
[12] K.K. Deng, X.J. Wang, C.J. Wang, J.Y. Shi, X.S. Hu, K. Wu, Mater. Sci. Eng. A 553 (2012) 74−79.
[13] W.S. Miller, F.J. Humphreys, Scr. Metal. Mater. 25 (1991) 33−38.
[14] Y. Yang, J. Lan, X.C. Li, 380, Mater. Sci. Eng. A (2004) 378−383.
[15] S.F. Hassan, M. Gupta, Mater. Sci. Tech. 20 (2005) 1383−1388.
[16] K.K. Deng, X.J. Wang, W.M. Gan, Y.W. Wu, K.B. Nie, K. Wu, M.Y. Zheng, H.G. Brokmeier, Mater. Sci. Eng. A 528 (2011) 1707−1712.